

# Mechanical and Rheological Properties of PP/SEBS/OMMT Ternary Composites

Feng-Hua Su, Han-Xiong Huang

Center for Polymer Processing Equipment and Intellectualization, College of Mechanical and Automotive Engineering, South China University of Technology, Guangzhou 510641, People's Republic of China

Received 18 July 2008; accepted 9 December 2008

DOI 10.1002/app.29875

Published online 24 February 2009 in Wiley InterScience (www.interscience.wiley.com).

**ABSTRACT:** The microstructure and mechanical properties of polypropylene (PP)/OMMT binary nanocomposites and PP/styrene-6-(ethylene-co-butylene)-6-styrene triblock copolymer (SEBS)/OMMT ternary nanocomposites were investigated using X-ray diffraction (XRD), transmission electron microscopy (TEM), and rheology and electromechanical testing machine. The results show that the organoclay layers are mainly intercalated and partially exfoliated in the PP-based nanocomposites. The additions of SEBS and OMMT have no significant effect on the crystallization behavior of PP. At the same time, it can be concluded that the polymer chains of PP and SEBS have intercalated into the organoclay layers and increase the gallery distance after blending process based on the analytical results from TEM, XRD, and rheology, which result in the form of a percolated nanostructure in the PP-based nanocomposites. The results of mechanical properties

show that SEBS filler greatly improve the notched impact strength of PP, but with the sacrifice of strength and stiffness. OMMT can improve the strength and stiffness of PP and slightly enhance the notched impact strength of PP/PP-g-MA. In comparison with neat PP, PP/OMMT, and PP/SEBS binary composites, notched impact toughness of the PP/SEBS/OMMT ternary composites significantly increase. Moreover, the stiffness and strength of PP/SEBS/OMMT ternary nanocomposites are slightly enhanced when compared with neat PP. It is believed that the synergistic effect of both SEBS elastomer and OMMT nanoparticles account for the balanced mechanical performance of the ternary nanocomposites. © 2009 Wiley Periodicals, Inc. *J Appl Polym Sci* 112: 3016–3023, 2009

**Key words:** PP/SEBS/OMMT ternary composites; mechanical properties; rheological properties

## INTRODUCTION

In recent years, polymer-layered silicate nanocomposites have drawn a lot of attention because of their academic and industrial importance.<sup>1–4</sup> The PA6/clay nanocomposite was first synthesized by a Toyota research group.<sup>1,2</sup> Polymer/clay nanocomposites can dramatically improve the mechanical reinforcement<sup>3,4</sup> and high-temperature durability,<sup>5</sup> provide enhanced barrier properties,<sup>6</sup> and reduce flammability.<sup>7</sup> The optimal performance of such composites is achieved when the clay fillers are uniformly dispersed in the polymer matrix. The nanocomposites are mainly prepared by two methods: *in situ* polymerization and melt blending. The melt blending is the dominating method to develop the polymer nanocomposites because this method can be easily put into practice in industries.

Polypropylene (PP) is one of the most widely used polyolefin polymers because of its advantages such as low density, low cost, high softening points, and easy processing. Moreover, great attentions had been paid to the PP/organoclay nanocomposites in the past decade.<sup>8–10</sup> It was reported that the addition of organoclay greatly improved the mechanical and thermal properties of PP.<sup>9–11</sup> However, further investigations showed that an obvious disadvantage of PP and PP/clay nanocomposites existed. This major deficiency was due to a low impact resistance, particularly at low temperatures, which was caused by its relatively high glass transition temperature ( $T_g$ ) of PP. To overcome this problem, the addition of an elastomer was an appropriate way for toughening the PP. Therefore, in the past decades, the toughening of PP with elastomer always was a popular research topic in the plastic modification field.<sup>12–15</sup> Thermoplastic elastomers have formed a new class of polymeric materials that have large number of applications because of their unique combination of both mechanical properties and process ability. Among the thermoplastic elastomers, the triblock copolymer was a special kind. Typical examples were styrene-*b*-butylenes-*b*-styrene (SBS), styrene-*b*-isoprene-styrene (SIS), and styrene-6-(ethylene-co-butylene)-6-styrene triblock copolymer (SEBS). SEBS

Correspondence to: F.-H. Su (fhsu@scut.edu.cn).

Contract grant sponsor: Research Fund for the Doctoral Program of Higher Education; contract grant number: 200805611099.

Contract grant sponsor: China Postdoctoral Science Foundation; contract grant number: 20080440749.

**TABLE I**  
**Materials**

Materials	Brand	Supplier	Characteristics
PP	EPS30R	Maomin Petroleum Chemical, Maomin, China	Density = 0.95 g/cm <sup>3</sup> ; MFI = 1.8 g/10 min
PP-g-MA	GPM200L	Ningbo New Materials, Ninbo, China	The content of MA = 1.0%; MFI = 28.4 g/10 min
SEBS	E1818	Kraton Polymers	The content of styrene = 33%; tensile strength = 5500 MPa; MFI < 1
OMMT	DK-1N	Zhejiang FengHong Clay Chemicals, Jiaxin, China	OMMT was organically modified through ion-exchange reaction with octadecylammonium; fully dispersed thickness of clay platelet about 25 nm; purified smectite content = 96–98%.

was the hardest and most resistant to degradation among the three thermoplastic elastomers. By blending PP with SEBS, the mechanical and processing properties of PP have been greatly improved.<sup>14,15</sup> However, elastomer toughening could not avoid decreasing rigidity and strength of the PP at the time of achieving an ideal toughening effect. To overcome the shortcoming and achieve an optimum balance of impact strength and stiffness, the ternary polymer composites composed of PP, elastomer, and inorganic filler were developed.<sup>16–20</sup> In this work, the ternary nanocomposites based on PP, SEBS, and OMMT were prepared to achieve the optimum balance of impact strength and stiffness of PP.

The ternary nanocomposites comprising PP, organoclay, and elastomer were usually examined from the aspect of mechanical properties and microstructure.<sup>21–23</sup> It is well known that the macroscale properties of polymer–clay nanocomposites are dominantly determined by the microscale structure of the composites. Many researchers have paid more attention to the dispersion of clay layers and morphology of the materials to understand the mechanism of the polymer–clay layers' interaction and also the connections between the macroscopic properties and the microscopic structures. X-ray diffraction (XRD), transmission electron microscopy (TEM), and rheology were extensively used to characterize the microstructure of polymer nanocomposites.<sup>23–26</sup>

In this study, we focused our attention mainly on the mechanical properties, microstructure, and the relation between the macroproperties and microstructure of the PP/SEBS/OMMT ternary nanocomposites. The microstructure of the composites and the dispersion of clay in composites were illustrated with the help of XRD, TEM, and rheology, which have been extensively used to decipher these questions.

## EXPERIMENT

### Materials

The materials used for the preparation of PP/SEBS/OMMT composites are listed in Table I. PP, SEBS, maleic anhydride-grafted polypropylene (PP-g-MA),

and OMMT used in this study were commercially available.

### Preparation of the composites

First, a batch of pellets with the composition of PP/PP-g-MA/OMMT (90/10/10 by weight) and another batch of pellets with the composition of PP/PP-g-MA (90/10 by weight) were melt-blended. Then, another series of PP/PP-g-MA/OMMT/SEBS (90/10/*x*/*y* by weight, *x* = 0, 0.5, 1, 3, 5, 7; *y* = 0, 5, 15, 25) composites were prepared through adding PP/PP-g-MA (90/10) and SEBS to dilute the as-prepared composites (PP/PP-g-MA/OMMT = 90/10/10), and then melt-blended. The compositions are shown in Table II. These blends were prepared by TE35 corotating twin-screw extruder. The temperatures of the extruder were maintained at 180, 200, 210, 215, 215, and 210°C from hopper to die, and the screw speed was 100 r/min in the blends. The pellets after dried for 24 h at 80°C in oven were injected into standard bars for mechanical tests with CJ-150M2 injection-molding machine at 210°C.

### Measurements and characterization

X-ray diffraction and transmission electron microscopy analysis

XRD experiments were carried out with a Rigaku (Japan) D/max 1200 diffractometer. The X-ray

**TABLE II**  
**Compositions of the PP-Based Composites**

Abbreviation	Composition			
	PP	PP-g-MA	OMMT	SEBS
C1	100	0	0	0
C2	90	10		
C3	90	10	0	15
C4	90	10	5	0
C5	90	10	0.5	15
C6	90	10	1	15
C7	90	10	3	15
C8	90	10	5	15
C9	90	10	7	15
C10	90	10	5	5
C11	90	10	5	25

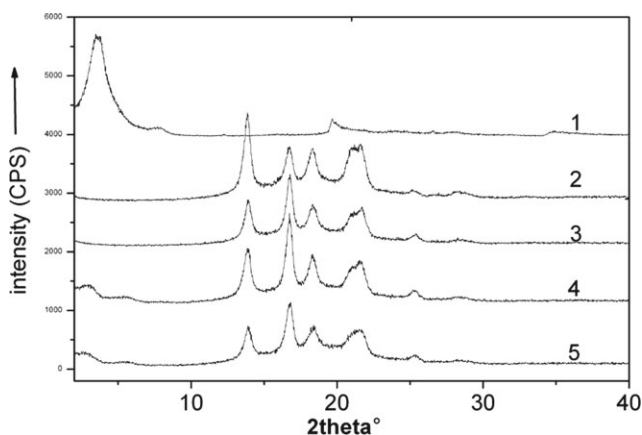


**Figure 1** XRD patterns of OMMT (1), C1 (2), C3 (3), and nanocomposites of C4 (4) and C8 (5).

beam was derived from nickel-filtered Cu K $\alpha$  ( $\lambda = 0.154$  nm) radiation in a sealed tube operated at 40 kV and 30 mA. The test samples were prepared by compression molding, and the test sample of OMMT was original commercial materials. The experiments were performed in the angle range  $2^\circ$ – $40^\circ$  at scanning step of  $0.02^\circ$ /s. These experiments were conducted to determine the dispersion of clay layers in the PP/OMMT or PP/SEBS/OMMT composites and the crystallization of PP in the composites.

The samples for TEM observation of nanocomposites were prepared by ultracryomicrotomy at  $-100^\circ\text{C}$  using an ultramicrotome equipped with a diamond knife. The microscopic study was conducted with a JEOL (Japan) (JEM-100CXII) TEM.

### Rheological measurement

All rheological experiments were conducted with a Bohlin Gemini 200 Rheometer equipped with a parallel-plate fixture (25-mm diameter). Disk samples were prepared by compression molding with a thickness of 2.0 mm and diameter of 25 mm. The gap between the two parallel plates was maintained at 1.75 mm for all rheological measurements. Storage modulus ( $G'$ ) and complex viscosity ( $\eta$ ) as a function of angular frequency ( $\omega$ ) ranging from 0.01 to 100 rad/s at  $190^\circ\text{C}$  were measured. A fixed strain of 1% was used to ensure that measurements were carried out within the linear viscoelastic range of the materials investigated.

### Mechanical measurement

The tensile and flexural properties were measured with Instron 5565 electromechanical testing machine with series IX control system. Tensile tests were carried out according to GB/T 1040-92 at a testing speed of 50 mm/min. Three-point flexural tests were performed in accordance to GB/T9341-2000. Tests

were conducted at a crosshead speed of 2.0 mm/min. According to GB1843-1996, Izod impact strength of notched samples was measured using an impact-testing machine, Pendulum Impact Tester CEAST 6967. At least five samples from each formulation were tested. All the tests were carried out at room temperature.

## RESULTS AND DISCUSSIONS

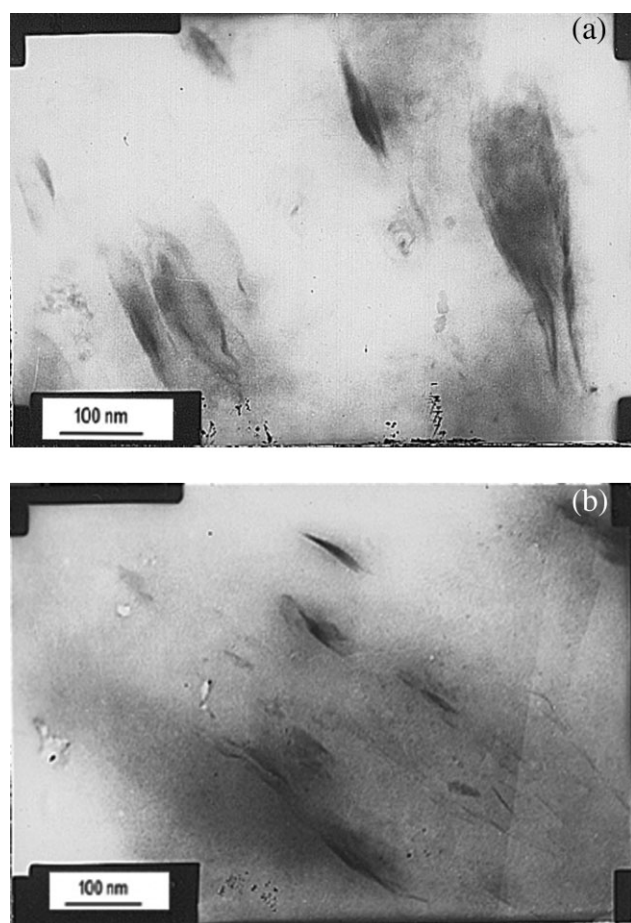
### The dispersion of OMMT in the nanocomposites

Figure 1 shows the XRD patterns of OMMT, neat PP (C1), PP/SEBS blend (C3), PP/OMMT binary nanocomposite (C4), and PP/SEBS/OMMT ternary nanocomposites (C8). C4 and C8 that were filled with 5-phr OMMT were selected as examples of PP/OMMT binary nanocomposites and PP/SEBS/OMMT ternary nanocomposites, respectively, to investigate the dispersion state of organoclay in them. From Figure 1, it can be seen that the silicate layer (001) reflection has peaks at  $2\theta = 3.76^\circ$ ,  $2.95^\circ$ ,  $2.62^\circ$  for OMMT, C4, and C8, respectively. The  $d_{001}$  spacing was calculated from Bragg's law. The interlayer distance of neat OMMT and nanocomposites for C4 and C8 are listed in Table III. The interlayer distance of nanocomposites is larger than that of the neat OMMT. This shows that the polymer chains including PP and SEBS does intercalate into the organoclay layers and increase the gallery distance of OMMT through the blending process. Moreover, it can be seen that interlayer distance of C8 is larger than that of C4, which indicate that SEBS is beneficial to intercalate the organoclay layers and expand the basal spacing. These results are different from the report by Sun et al.<sup>23</sup> They investigated the dispersion of clay in PP/POE/OMMT ternary composites and found that the elastomer of POE did not significantly affect the intercalation and the exfoliation of PP/OMMT composites.

In the small angle region of XRD patterns, there are significance difference between the curves of OMMT and those of these nanocomposites. Not only the position and the shape of these diffraction peaks are shifting and breaking but also the intensities are greatly reduced, which indicate that the state of organoclay in the nanocomposites is

**TABLE III**  
Interlayer Spacing of OMMT and Hybrid Materials from XRD

Sample	$2\theta$ ( $^\circ$ )	$d_{001}$ (nm)
OMMT	3.96	2.21
C4	2.88	3.05
C8	2.57	3.43



**Figure 2** Transmission electron microscopy micrographs of (a) C4 and (b) C8.

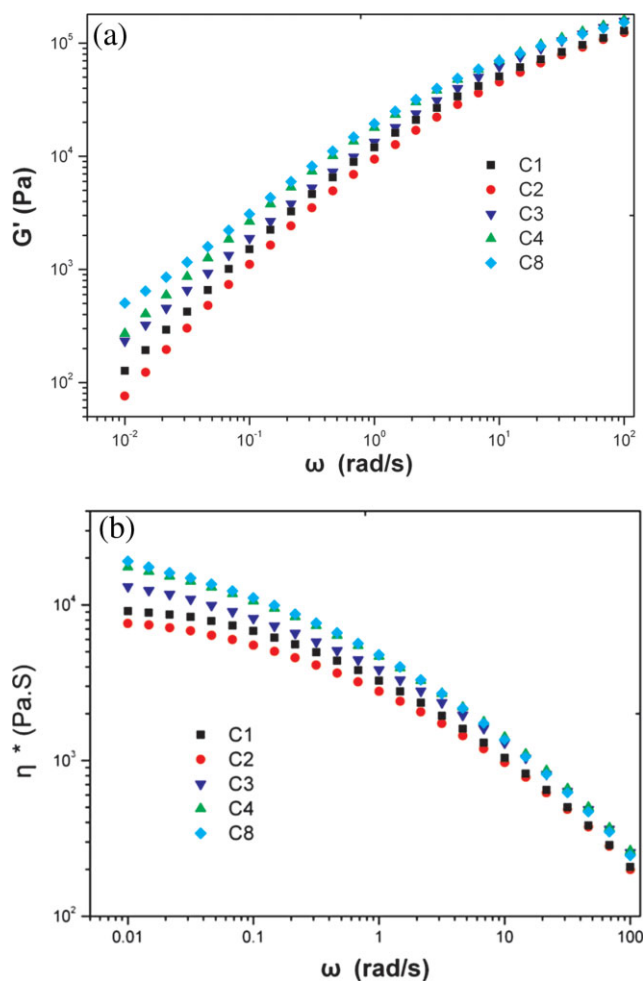
dramatically different from the neat organoclay. At the same time, the peak position and shape of C1, C3, C7, and C8 in  $10^{\circ}$ – $40^{\circ}$  are almost the same, which indicate there is no big difference in the crystal form of PP. Namely, the addition of SEBS and OMMT has no big effect on the crystallization behavior of PP.

Figure 2 shows the TEM image of C4 and C8. From Figure 2(a), it can be seen that, with the effects of shearing force, most of OMMT are intercalated and even partially exfoliated by polymer chains. However, a few OMMT still maintains ordered stacks in the PP matrix. The OMMT stacks with thickness of about 10–50 nm are dispersed in PP matrix. As shown in Figure 2(b), it can be seen that OMMTs in PP/SEBS/OMMT system possess a larger  $d$ -spacing and a thinner sheet thickness than those in PP/OMMT system. Therefore, it can be concluded that SEBS can easily intercalate in silicate layer and expand the basal spacing. Moreover, it can be seen that OMMT are almost intercalated and exfoliated in the PP/SEBS/OMMT ternary composites (C8) by polymer chains of PP and SEBS, and

the stacked OMMT is very few. The thickness of the exfoliated OMMT flack is below 10 nm. As a result, it can be confirmed that PP/SEBS/OMMT ternary nanocomposites are formed, as the individual silicates are well-dispersed in the polymer matrix. Chen et al.<sup>15</sup> reported a similar observation for PP/SEBS/OMMT nanocomposites that the SEBS can easily intercalate in silicate layer and expand the basal spacing, which might be attributed to the fact that OMMT has a higher affinity to SEBS.

### Rheological behavior of the nanocomposites

Rheological measurements are very sensitive to the shape, size, and the dispersion of fillers in the nanocomposites, and therefore an oscillatory shear measurement is used to characterize the dynamic rheological properties of PP/OMMT binary nanocomposites and PP/SEBS/OMMT ternary nanocomposites. The dynamic frequency sweep measurements of PP (C1), PP/PP-*g*-MA (C2), PP/SEBS blend (C3), PP/OMMT binary nanocomposite (C4), and PP/SEBS/OMMT ternary nanocomposites (C8) at  $190^{\circ}\text{C}$  are shown in Figure 3. It can be seen that the storage modulus and complex viscosity of PP/PP-*g*-MA (C2) is lower than that of neat PP (C1), indicating that the addition of PP-*g*-MA decreases the elastic behavior and increases the viscosity of PP. This result might be owing to the intrinsic viscous/elastic characteristics of commercial PP-*g*-MA. It can be seen that the storage modulus and complex viscosity of C3, C4, and C8 are larger than that of C2 and C1, especially in the low frequency region. The storage modulus and complex viscosity of the nanocomposite of C8 is the largest among all investigated cases in the low-frequency region. The storage modulus of PP increase in the low-sweep frequency region as it was filled with OMMT, which agrees well with the report by Wang et al.<sup>27</sup> Besides the neat PP, the modulus and complex viscosity of PP/SEBS also increase as it filled with OMMT. These results could be attributed to the polymer chains of PP and SEBS that intercalate into the organoclay layers and increase the gallery distance after blending process, and the percolated nanostructure has been formed in the binary and ternary nanocomposites. The complex viscosity of PP and PP/SEBS increases as it filled with OMMT, which can be attributed to the partly exfoliated and intercalated silicate layers with restrict the melt flow of the blend matrix. The similar results have been reported by Ma et al.<sup>18</sup> They found that nano- $\text{CaCO}_3$  in PP/PEO/nano- $\text{CaCO}_3$  ternary composite can also restrict the melt flow of the PP/PEO blend. The change of slopes for storage modulus and complex viscosity versus frequency curve in low-frequency region is more obvious after SEBS have been added in PP/OMMT, which



**Figure 3** Storage modulus (a) and complex viscosity (b) versus angular frequency at 190°C for neat PP (C1), PP/PP-*g*-MA (C2), PP/SEBS blend (C3), PP/OMMT (C4), and PP/SEBS/OMMT nanocomposites (C8). [Color figure can be viewed in the online issue, which is available at [www.interscience.wiley.com](http://www.interscience.wiley.com).]

indicated that SEBS has played an additional role in the percolated nanostructure formation in PP/SEBS/OMMT nanocomposites during the blending process. The structures of PP/PEO/OMMT ternary composites have been investigated by Sun et al.<sup>23</sup> They also confirmed that PEO can interact with the three-dimensional filler network, which helped to influence rheological behavior of PP/POE/OMMT ternary composites. In our research system, probably SEBS interacts with the intercalated nanostructure, which help to influence the low-frequency behavior of PP/SEBS/OMMT nanocomposites. The analytical results from rheology agree well with the results from the XRD and TEM.

Figure 4 shows the variation of storage modulus versus angular frequency of PP/SEBS/OMMT ternary nanocomposites with increasing OMMT content and with increasing SEBS content, respectively, at 190°C. In these cases of the increase of OMMT con-

tent in PP/SEBS/OMMT ternary nanocomposites, the content of SEBS is fixed at 15 phr. With the increase of SEBS content, the content of OMMT is fixed at 5 phr. As shown in Figure 4(a), the slope of  $G'$  vs.  $\omega$  curve in the terminal region become smaller with increasing OMMT content for PP/SEBS/OMMT nanocomposites. The system exhibit a pseudo solid-like behavior in low-frequency region when a proper content OMMT has been added in the PP/SEBS. This phenomenon might be attributed to the fact that the clay layer are unable to free rotation because of physical jamming and connection, which lead to the percolated nanostructure more easily formed with the increase of the organoclay content.<sup>23</sup>

As shown in Figure 4(b), the storage modulus of PP/SEBS/OMMT in the frequency region increase with the increase of SEBS content up to 15 phr, which indicate that SEBS does participate in the formation of the percolated nanostructure of the nanocomposites. With the increase of SEBS content, the phase-separated SEBS-rich domains, which might be either wrapping around the OMMT/PP-*g*-MA

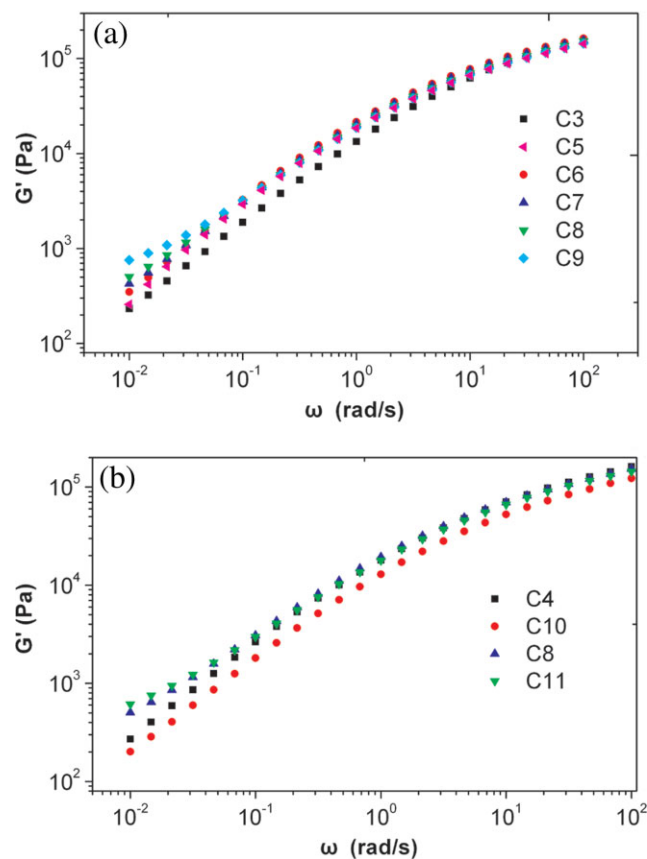


**Figure 4** Variation of storage modulus versus angular frequency of PP/SEBS/OMMT ternary nanocomposites with increasing OMMT content (a) and SEBS content (b) at 190°C. [Color figure can be viewed in the online issue, which is available at [www.interscience.wiley.com](http://www.interscience.wiley.com).]

structure or absorbing these structures on the domain surfaces, can easily promote the formation of a percolated nanostructure of the nanocomposites. However, as the content of SEBS is more than 15 phr, the storage modulus of the nanocomposites does not change obviously, indicating that a compact network structure in PP/SEBS/OMMT nanocomposites might have formed when SEBS content is over 15 phr.

### Mechanical properties of nanocomposites

Figure 5 shows the mechanical properties of initial PP and its composites including PP/PP-g-MA (C2),

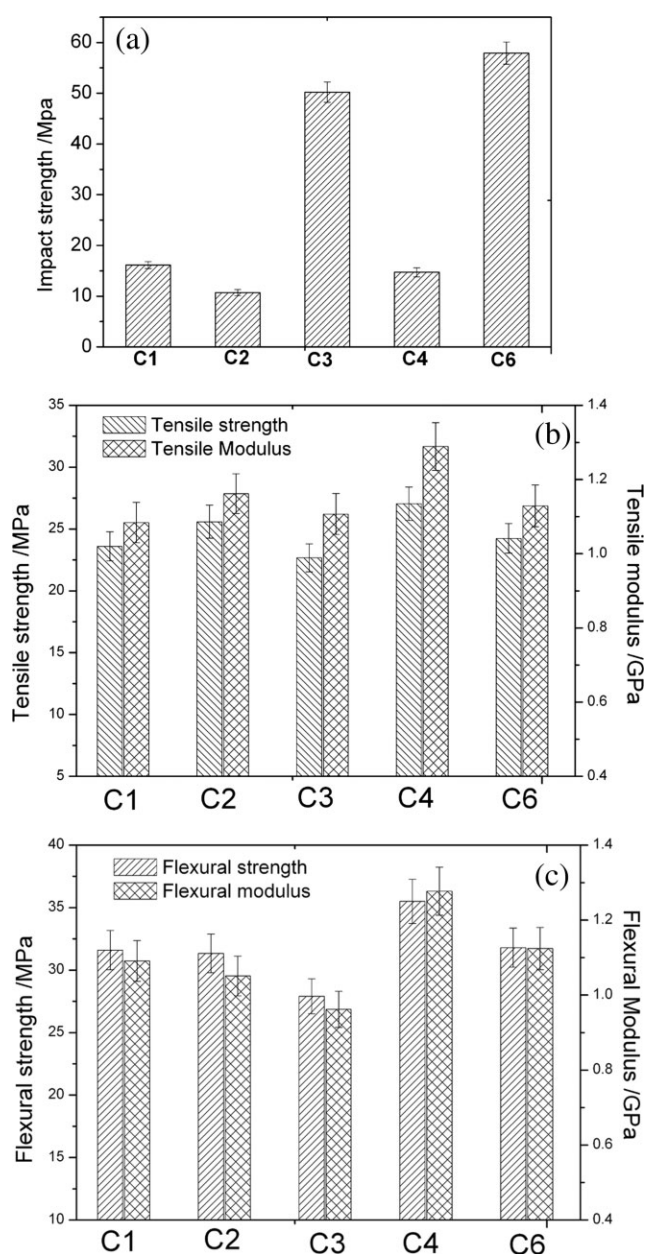


**Figure 5** Mechanical properties of PP and its composites at room temperature.

PP/SEBS (C3), PP/OMMT (C4) binary composites, and PP/SEBS/OMMT (C6) ternary composites. It can be observed that the addition of PP-g-MA compatibilizer into PP leads to a great decrease of the impact strength and a slight decrease of the flexural strength and modulus, but a slight increase of the tensile strength and modulus of PP, which is attributed to the intrinsic mechanical properties of commercial PP-g-MA. In comparison with PP/PP-g-MA (C2), the addition of 5-phr OMMT (C4) greatly improves the stiffness and strength and increases the impact strength of PP/PP-g-MA. In contrast, the impact strength of PP is rapidly increased as it was filled with 15-phr SEBS (C3), but with the sacrifice of the decrease of strength and stiffness. Further inclusion of 1-phr OMMT into PP/SEBS leads to much higher impact strength for the PP/SEBS/OMMT ternary nanocomposites (C5). Moreover, the tensile strength and flexural strength and the tensile modulus and flexural modulus of PP/SEBS/OMMT ternary nanocomposites are much higher than those of PP/SEBS blend. The OMMT are dispersed in PP or PP/SEBS matrix on the nanometer scale and most of OMMT are intercalated by the polymer chain of PP and SEBS, which corresponds to the formation of percolated nanostructure in the PP/OMMT and PP/SEBS/OMMT nanocomposites. As shown in many works,<sup>18,28</sup> this percolated nanostructure can improve the mechanical properties of PP-based composites. At the same time, the silicate layer orientation may also contribute to the observed reinforcement effects.

Figure 6 shows the effect of OMMT content on the mechanical properties of PP/SEBS/OMMT (100/15/ $x$ ,  $x = 0, 0.5, 1, 3, 5, 7$ ) ternary composites with a given SEBS content at 15 phr. It can be seen from Figure 6(a) that the impact strength of PP/SEBS/OMMT (100/15/ $x$ ) ternary composites increases with the increase of OMMT content up to 1 phr and then decreases with the further increase of OMMT content. The tensile strength and tensile modulus and the flexural strength and flexural modulus of the PP/SEBS/OMMT ternary nanocomposites are much higher than that of PP/SEBS blend as it was filled with different content OMMT, which is attributed to the reinforcing feature of OMMT. The impact strength of PP/SEBS/OMMT ternary nanocomposites filled with 1-phr OMMT is higher than that of the PP/SEBS blend. When OMMT was added to PP/SEBS, the percolated nanostructure formed owing to the intercalation of the PP and SEBS macromolecular chain, which has been illustrated with the help of TEM, XRD, and rheology. The formed percolated nanostructure in PP/SEBS/OMMT ternary nanocomposites can improve the impact strength of the composites. As high content of OMMT incorporated in the composites, the

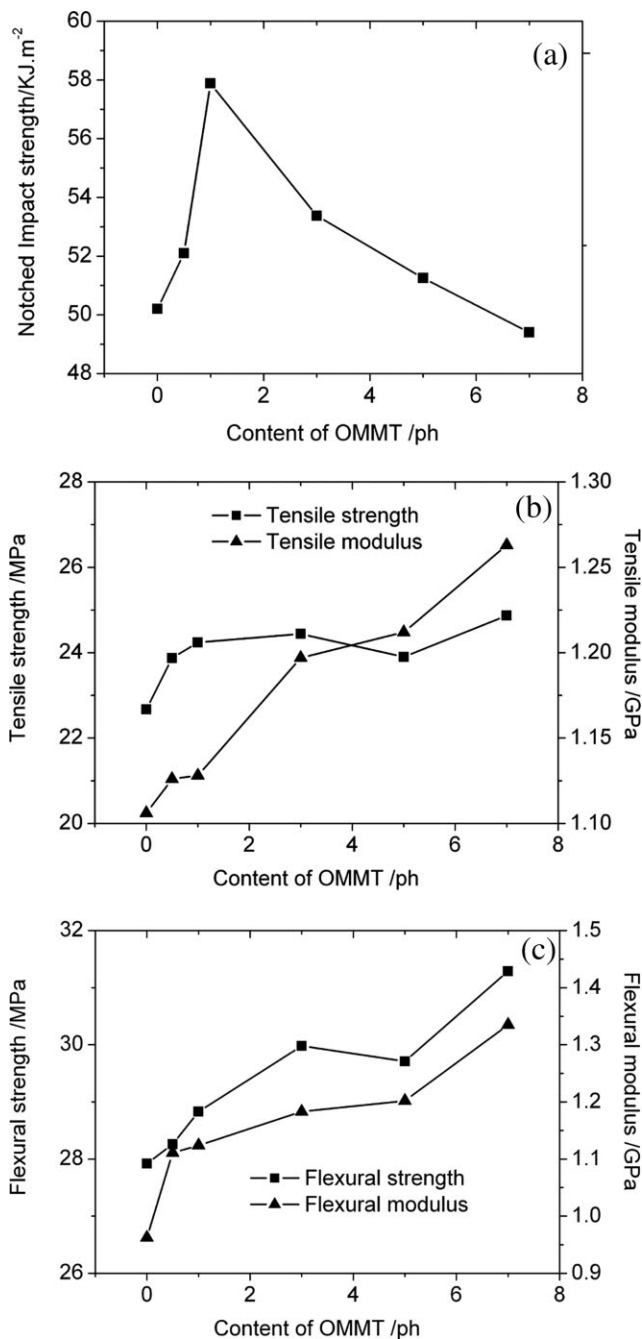


**Figure 6** Effect of OMMT content on the mechanical properties of PP/SEBS/OMMT (100/15/ $x$ ,  $x = 0, 0.5, 1, 3, 5, 7$ ) ternary nanocomposites.

agglomeration might take place that correspond to the decreased impact strength of the ternary nanocomposite with the further increase of OMMT. The impact strength of PP/SEBS/OMMT ternary nanocomposites with different composition is much higher than that of the neat PP. However, the strength and the stiffness of the ternary nanocomposites are slightly enhanced when compared with the neat PP, which is due to the synergistic effect of SEBS and the reinforcing feature of the OMMT.

Figure 7 shows the effect of SEBS content on the mechanical properties of PP/SEBS/OMMT with a given OMMT content at 5 phr. We can find that the impact strength of PP/SEBS/OMMT (100/ $x$ /5) increase rapidly with increasing SEBS content. This behavior is similar to the cases of polymers toughened with rubber. However, the flexural strength and tensile strength of the ternary nanocomposites rapidly decrease with the increase of SEBS content. These results agree well with other reports that showed elastomer can improve the impact strength of PP but with the sacrifice of tensile and flexural strength.<sup>29,30</sup>

In conclusion, SEBS as filler can greatly improve the impact strength of PP, but with the sacrifice of strength and stiffness. OMMT can improve the strength and stiffness but slightly improve the impact strength of PP. Ternary polymer nanocomposites containing soft elastomer and rigid nanoparticle filler have long been the subject of studies aiming to achieve an optimum balance of impact strength and stiffness. In comparison with neat PP, PP/OMMT, and PP/SEBS binary composites, notched impact toughness of the PP/SEBS/OMMT ternary

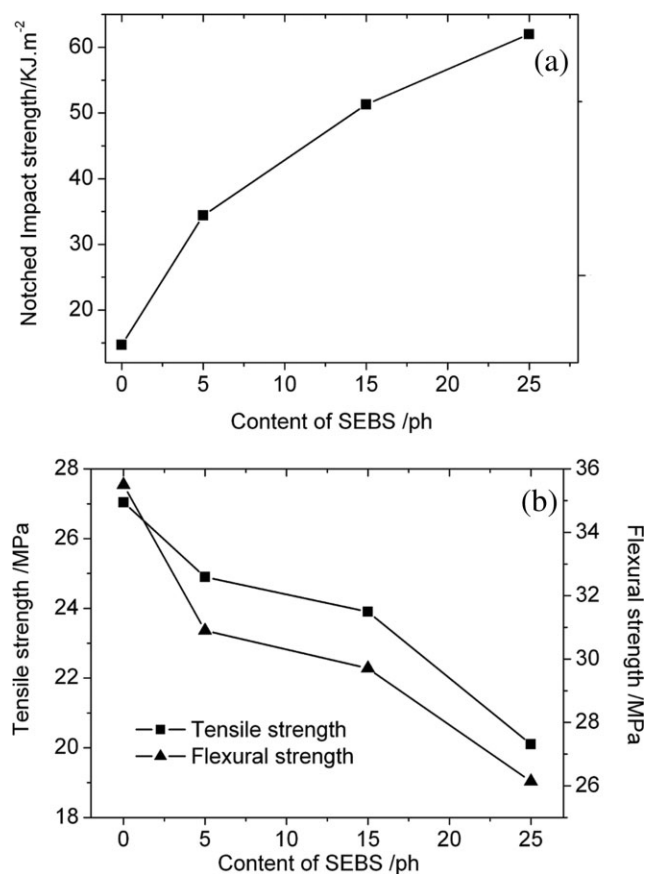


**Figure 7** Effect of SEBS content on the mechanical properties of PP/SEBS/OMMT (100/ $x$ /5,  $x = 0, 5, 15, 25$ ) ternary nanocomposites.

composites are significantly enhanced. Meanwhile, the stiffness and tensile strength of PP/SEBS/OMMT ternary nanocomposites are slightly enhanced. It is believed that the synergistic effect of both SEBS elastomer and OMMT nanoparticles should account for the balanced mechanical performance of the ternary nanocomposites.

### CONCLUSION

The percolated nanostructure in PP/OMMT binary composites and PP/SEBS/OMMT ternary composites has been formed after melt-blending processes, which are demonstrated by XRD, TEM, and rheology. The organoclay layers were mainly intercalated and partially exfoliated in the PP/OMMT binary nanocomposites and PP/SEBS/OMMT ternary nanocomposites. At the same time, it can be concluded that the polymer chains of PP and SEBS intercalated into the organoclay layers and increased the gallery distance after blending process, which result in the formation of the percolated nanostructure in the ternary nanocomposites. Moreover, it has been proved that SEBS has played an additional role in the formation of percolated nanostructure in PP/SEBS/OMMT ternary nanocomposites because the polymer chain of SEBS can easily intercalate the organoclay layers and expand the basal spacing of OMMT.

SEBS as filler can greatly improve the notched impact strength of PP, but with the sacrifice of strength and stiffness. OMMT can improve the strength and stiffness of PP and slightly enhance the notched impact strength of PP/PP-g-MA. In comparison with neat PP, PP/OMMT, and PP/SEBS binary composites, notched impact toughness of PP/SEBS/OMMT ternary composites are significantly enhanced. Meanwhile, the stiffness and strength of PP/SEBS/OMMT ternary nanocomposites are slightly enhanced. It is believed that the synergistic effect of both SEBS elastomer and OMMT nanoparticles should account for the balanced mechanical performance of the ternary nanocomposites.

### References

1. Usuki, A.; Kojijima, Y.; Kawasumi, M.; Okada, A.; Fukushima, Y.; Kurauchi, T. *J Mater Res* 1993, 8, 1185.
2. Usuki, A.; Kojijima, Y.; Kawasumi, M.; Okada, A.; Fukushima, Y.; Kurauchi, T. *J Mater Res* 1993, 8, 1179.
3. Kawasumi, M.; Hasegawa, N.; Kato, M.; Usuki, A.; Okada, A. *Macromolecules* 1997, 30, 6333.
4. Giannelis, E. P. *Adv Mater* 1996, 8, 29.
5. Koo, C. M.; Kim, M. J.; Choi, M. H.; Kim, S. O.; Chung, I. J. *J Appl Polym Sci* 2003, 88, 1526.
6. Bharadwaj, R. K. *Macromolecules* 2001, 34, 1989.
7. Kim, S.; Wikie, C. A. *Polym Adv Technol* 2008, 19, 496.
8. Hasegawa, N.; Kawasumi, M.; Kato, M.; Usuki, A.; Okada, A. *J Appl Polym Sci* 1998, 67, 87.
9. Hasegawa, N.; Okamoto, H.; Kato, M.; Usuki, A. *J Appl Polym Sci* 2000, 78, 1918.
10. Morgan, A. B.; Harris, J. D. *Polymer* 2003, 44, 2113.
11. Nam, P. H.; Maiti, P.; Okamoto, M.; Kotaka, T.; Hasegawa, N.; Usuki, A. *Polymer* 2001, 42, 9633.
12. Cai, H.; Luo, X.; Ma, D.; Wang, J.; Tan, H. *J Appl Polym Sci* 1999, 71, 93.
13. Fan, Z.; Zhang, Y.; Xu, J.; Wang, H.; Feng, L. *Polymer* 2001, 42, 5559.
14. Ohlsson, B.; Tdrnell, B. *Polym Eng Sci* 1996, 36, 1547.
15. Chen, H. L.; Zhou, L. Y.; Ye, Q.; Chen, J. *Modem Plast Process Appl* 2004, 16, 42 (in Chinese).
16. Yang, H.; Zhang, X. Q.; Qu, C.; Li, B.; Zhang, L. J.; Zhang, Q.; Fu, Q. *Polymer* 2007, 48, 860.
17. Ma, C. G.; Zhang, M. Q.; Rong, M. Z. *J Appl Polym Sci* 2007, 103, 1578.
18. Ma, C. G.; Mai, Y. L.; Rong, M. Z.; Ruan, W. H.; Zhang, M. Q. *Compos Sci Technol* 2007, 67, 2997.
19. Long, Y.; Shanks, R. A. *J Appl Polym Sci* 1996, 61, 1877.
20. Wang, J.; Tung, J. F.; Fuad, M. Y. A.; Hornsby, P. R. *J Appl Polym Sci* 1996, 60, 1425.
21. Maiti, M.; Bandyopadhyay, A.; Bhowmick, A. K. *J Appl Polym Sci* 2006, 99, 1645.
22. Tjong, S. C.; Bao, S. P.; Liang, G. D. *J Polym Sci Part B: Polym Phys* 2005, 43, 3112.
23. Sun, T. C.; Dong, X.; Du, K.; Wang, K.; Fu, Q.; Han, C. C. *Polymer* 2008, 49, 588.
24. Koo, C. M.; Kim, S. O.; Chung, I. J. *Macromolecules* 2003, 36, 2748.
25. Marchant, D.; Jayaraman, K. *Ind Eng Chem Res* 2002, 41, 6402.
26. Galgali, G.; Ramesh, C.; Lele, A. *Macromolecules* 2001, 34, 852.
27. Wang, K.; Liang, S.; Zhao, P.; Qu, C.; Tan, H.; Du, R. N.; Fu, Q. *Acta Mater* 2007, 55, 3143.
28. Ding, C.; Jia, D. M.; He, H.; Guo, B. C.; Hong, H. Q. *Polym Test* 2005, 24, 94.
29. Yin, J.; Zhang, Y.; Zhang, Y. X. *J Appl Polym Sci* 2005, 98, 957.
30. Wu, S. J. *J Appl Polym Sci* 1988, 35, 549.